

Modeling interactions between voltage-gated Ca^{2+} channels and KCa1.1 channels

Jordan DT Engbers¹, Gerald W Zamponi², and Ray W Turner^{1,2}

¹Department of Cell Biology & Anatomy; Hotchkiss Brain Institute; University of Calgary; Calgary, AB Canada; ²Department of Physiology & Pharmacology; Hotchkiss Brain Institute; University of Calgary; Calgary, AB Canada

High voltage-activated (HVA) Cav channels form complexes with KCa1.1 channels, allowing reliable activation of KCa1.1 current through a nanodomain interaction. We recently found that low voltage-activated Cav3 calcium channels also create KCa1.1-Cav3 complexes. While coimmunoprecipitation studies again supported a nanodomain interaction, the sensitivity to calcium chelating agents was instead consistent with a microdomain interaction. A computational model of the KCa1.1-Cav3 complex suggested that multiple Cav3 channels were necessary to activate KCa1.1 channels, potentially causing the KCa1.1-Cav3 complex to be more susceptible to calcium chelators. Here, we expanded the model and compared it to a KCa1.1-Cav2.2 model to examine the role of Cav channel conductance and kinetics on KCa1.1 activation. As found for direct recordings, the voltage-dependent and kinetic properties of Cav3 channels were reflected in the activation of KCa1.1 current, including transient activation from lower voltages than other KCa1.1-Cav complexes. Substantial activation of KCa1.1 channels required the concerted activity of several Cav3.2 channels. Combined with the effect of EGTA, these results suggest that the Ca^{2+} domains of several KCa1.1-Cav3 complexes need to cooperate to generate sufficient $[\text{Ca}^{2+}]_i$, despite the physical association between KCa1.1 and Cav3 channels. By comparison, Cav2.2 channels were twice as effective at activating KCa1.1 channels and a single KCa1.1-Cav2.2 complex would be self-sufficient. However, even

though Cav3 channels generate small, transient currents, the regulation of KCa1.1 activity by Cav3 channels is possible if multiple complexes cooperate through microdomain interactions.

Introduction

Calcium-dependent potassium (K_{Ca}) channels are known to form complexes with voltage-gated calcium (Ca^{2+}) sources. These interactions are important in linking the voltage-dependent and temporal properties of Ca^{2+} influx to K_{Ca} channel activation, allowing the K_{Ca} channel to respond rapidly and effectively to Ca^{2+} channel activity. Big conductance K_{Ca} (KCa1.1) channels are both voltage- and Ca^{2+} -dependent and were known to complex with high voltage-activated (HVA) Ca^{2+} channels.¹⁻³ Recently, we showed that KCa1.1 channels also form a physical complex with low voltage-activated (LVA) Cav3 T-type Ca^{2+} channels, as shown through coimmunoprecipitation.⁴ Interaction with Cav3 Ca^{2+} channels was shown to allow KCa1.1 channels to be activated at voltages as low as -70 mV, 30 – 40 mV lower than the activation threshold seen for KCa1.1-Cav2.1 complexes.¹ This low-voltage KCa1.1 activity, which extended into the subthreshold region, was seen in both a heterologous expression system and neurons of the medial vestibular nucleus (MVN).⁴

While determining the properties of the KCa1.1-Cav3.2 complex, we compared the effectiveness of 2 different Ca^{2+} chelators, EGTA and BAPTA, at disrupting Ca^{2+} -dependent activation to help distinguish

Keywords: ion channel complex; KCa1.1; BK; Cav3; Cav2.2

*Correspondence to: Ray W Turner;
Email: rwtturner@ucalgary.ca

Submitted: 07/18/2013;

Accepted: 07/18/13

<http://dx.doi.org/10.4161/chan.25867>

Addendum to: Rehak R, Bartoletti TM, Engbers JDT, Berecki G, Turner RW, Zamponi GW. Low voltage activation of KCa1.1 current by Cav3-KCa1.1 complexes. *PLoS One* 2013; 8:e61844; PMID:23626738; <http://dx.doi.org/10.1371/journal.pone.0061844>

between a nanodomain and microdomain interactions. It is understood that the ability to block a Ca^{2+} -dependent process by internal perfusion of BAPTA, but not EGTA, indicates an interaction between partners at the nanodomain level (20–50 nm). If, instead, the interaction is blocked by internal EGTA, it suggests an interaction with the Ca^{2+} source at the level of a microdomain (> 50 nm).⁵ Coimmunoprecipitation between KCa1.1 and Cav3 channels even from lysates of tsA-201 cells expressing only the α subunits revealed a close physical association expected for a nanodomain interaction. Yet internal EGTA was found to block Ca^{2+} -dependent activation of KCa1.1 current in either tsA-201 cells or MVN neurons, raising an apparent contradiction in the data set.

Activation of KCa1.1 channels requires an increase in the concentration of internal Ca^{2+} [Ca^{2+}]_i of 1–10 μM .^{1,6,7} We considered that the chelator test results might reflect the relative strength of Cav3 channels as a Ca^{2+} source, such that the transient Ca^{2+} current and relatively low conductance of Cav3 channels may reduce the ability to activate KCa1.1 channels. To test this we constructed a model of the KCa1.1-Cav3 interaction and found that multiple Cav3 channels are required to provide reliable activation of KCa1.1 channels, perhaps acting cooperatively over larger distances. Here, we expand on the model briefly presented in Rehak et al. (2013) to compare the properties of a KCa1.1-Cav3.2 complex to that of a model for KCa1.1 activation by the HVA Cav2.2 (N-type) Ca^{2+} channel.

Methods

The KCa1.1-Cav complexes were modeled using systems of differential equations describing the activation and inactivation of the included ion channels, as well as diffusion of Ca^{2+} from the Ca^{2+} source.^{8–11}

I_{CaT} activation:

$$m_{\infty} = \frac{1}{1 + e^{-\frac{V+44.3}{-5.5}}}, \quad \frac{dm}{dt} = \frac{m_{\infty} - m}{\tau_m}, \quad \tau_m = 7 \text{ ms}$$

(Equation 1)

I_{CaT} inactivation:

$$h_{\infty} = \frac{1}{1 + e^{\frac{V+64.2}{6.27}}}, \quad \frac{dh}{dt} = \frac{h_{\infty} - h}{\tau_h}, \quad \tau_h = 37 \text{ ms}$$

(Equation 2)

I_{CaN} activation:

$$m_{\infty} = \frac{1}{1 + e^{-\frac{V+21}{-7.2}}}, \quad \frac{dm}{dt} = \frac{m_{\infty} - m}{\tau_m}, \quad \tau_m = 4 \text{ ms}$$

(Equation 3)

I_{CaN} inactivation:

$$h_{\infty} = \frac{1}{1 + e^{\frac{V+78}{S}}}, \quad \frac{dh}{dt} = \frac{h_{\infty} - h}{\tau_h}, \quad \tau_h = 500 \text{ ms}$$

(Equation 4)

For all simulations, $E_{\text{Ca}} = 40$ mV and currents were calculated according to the Hodgkin–Huxley formalism. Simulations were constructed in Matlab R2007b using a fourth-order Runge-Kutta algorithm with a time step (dt) of 0.0001 ms. The maximum open probability (p_{max}) for Cav3 channels was set to 0.25¹⁰ and Cav2.2 channels to 0.8.⁸ To calculate calcium influx, single channel conductance was set to 1.7 pS for Cav3 channels ($\hat{g}_{\text{CaT}} = 1.7$ pS) and 2.8 pS for Cav2.2 channels ($\hat{g}_{\text{CaN}} = 2.8$ pS).¹² To simulate multiple Cav channels, \hat{g} was multiplied by the number of desired channels. The number of incoming calcium ions (N_{Ca}) was determined by:

$$N_{\text{Ca}} = \frac{\hat{g} \cdot m \cdot h \cdot p_{\text{max}} \cdot (V - E_{\text{Ca}})}{2F}$$

(Equation 5)

where F is the Faraday constant (9.649 · 10⁴ coulombs/mol).¹³

Ca^{2+} diffusion model

Ca^{2+} diffusion away from the Cav Ca^{2+} source was modeled through 10 hemispherical compartments. The following explicit equation was used to calculate diffusion¹³:

$$\frac{d[\text{Ca}^{2+}]_n}{dt} = D_{\text{Ca}} \frac{a_{n,n+1}}{V_n \delta_{n,n+1}} ([\text{Ca}^{2+}]_n - [\text{Ca}^{2+}]_{n+1})$$

(Equation 6)

where D_{Ca} is the diffusion coefficient for Ca^{2+} (0.220 $\mu\text{m}^2\text{ms}^{-1}$), $a_{n,n+1}$ is the surface area between the adjacent compartments, v_i is the volume of the first compartment, $\delta_{n,n+1}$ is the distance between compartments, and the term in the brackets represents the concentration gradient. The radius of the smallest compartment was 20 nm and the radius of each consecutive compartment was increased by 20 nm. The KCa1.1 channel was placed in a compartment n and its activation calculated based on $[\text{Ca}^{2+}]_n$, as described below. Therefore, the effect of Ca^{2+} on KCa1.1 channels could be observed for distances of up to 200 nm from the Ca^{2+} source by changing the compartment in which the KCa1.1 channel was located.

Large conductance Ca^{2+} -activated K⁺ channel model

The parameters for voltage- and Ca^{2+} -dependence of KCa1.1 channels previously described for Purkinje cells⁷ were used to develop a model of the KCa1.1 channel. The equation for τ was adapted from a previous model of a KCa1.1 channel.¹⁴ The Ca^{2+} -dependence for $V_{1/2}$ was adjusted to allow near maximal shift in $V_{1/2}$ with 10 μM [Ca^{2+}]_i.

The relationship between the $V_{1/2}$ of activation and Ca^{2+} concentration (in μM) can be described by the equation:

$$V_{1/2}([\text{Ca}^{2+}]) = -66 + 137e^{-0.3044[\text{Ca}^{2+}]} + 30.24e^{-0.0414[\text{Ca}^{2+}]}$$

(Equation 7)

The maximum voltage of p_{open} for a given voltage over all concentrations of Ca^{2+} is given by the equation:

$$p_{\text{max}}(V) = \left(\frac{1}{1 + e^{-(V+44.8)/0.074}} \right)$$

(Equation 8)

Using p_{max} and the dissociation constant of Ca^{2+} at a given voltage, K_D , the maximum p_{open} for a given [Ca^{2+}] is:

$$K_D(V) = 10.76e^{-0.01949V}$$

(Equation 9)

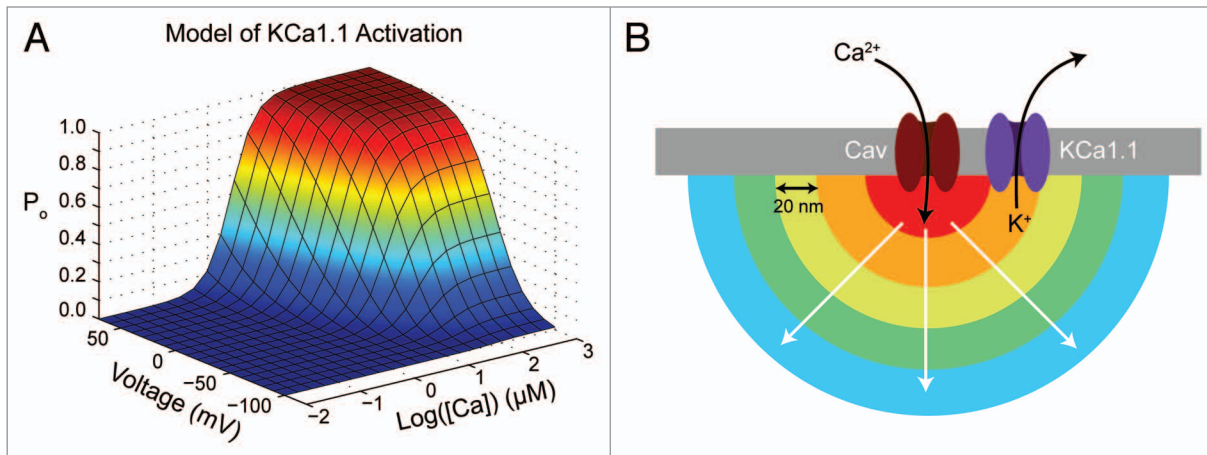


Figure 1. Illustration of KCa1.1-Cav model design. **(A)** The voltage – and Ca^{2+} -dependence of the KCa1.1 model is shown. Increasing $[Ca^{2+}]_i$ results in a left-shift in voltage-dependence of KCa1.1 activation with maximal shift between 10 and 100 μM . Maximum P_o is also Ca^{2+} -dependent and increases with increasing $[Ca^{2+}]_i$. **(B)** A diagram of the KCa1.1-Cav model showing the diffusion of Ca^{2+} through multiple hemispherical compartments. The KCa1.1 channel is placed in a compartment and its activation calculated according to the local $[Ca^{2+}]_i$.

$$p_o([Ca^{2+}]) = p_{max} \left(\frac{1}{\left(\frac{K_D}{[Ca^{2+}]^2} \right) + 1} \right)$$

(Equation 10)

Finally, the activation rates and time constant, τ , are:

$$\alpha_m = 25$$

(Equation 11)

$$\beta_m(V) = \frac{0.075}{e^{(V-V_{1/2})/10}}$$

(Equation 12)

$$\tau_m(V) = 18.06 - \frac{15.02}{1 + e^{(V-40)/-22.7}}$$

(Equation 13)

The differential equation to describe the activation variable of KCa1.1 channels, m , is therefore:

$$\frac{dm([Ca^{2+}], V)}{dt} = \frac{\alpha_m(p_o - m) - \beta_m m}{\tau_m}$$

(Equation 14)

This model generates a complex voltage- and Ca^{2+} -dependent relationship for KCa1.1 activation, as seen in Figure 1A. In particular, increasing $[Ca^{2+}]_i$ causes a hyperpolarized shift in KCa1.1 half-activation and increase in p_{max} consistent with physiological recordings of KCa1.1 channel properties.

Results

The distance between HVA Cav channels and KCa1.1 channels required to generate KCa1.1 activation and effects of Ca^{2+} chelators has been solved analytically in previous studies.^{5,15} Here, we were interested in modeling the effects of varying the interchannel distance between either HVA (Cav2.2) or LVA (Cav3.2) Ca^{2+} channels and KCa1.1 channels. In this way, we could determine how the properties of a Ca^{2+} source affect the voltage-dependence and temporal properties of KCa1.1 channel activation. The Cav-mediated Ca^{2+} source was modeled using 10 hemispherical compartments of increasing radii (20–200 nm; Fig. 1) and KCa1.1 channel activation was calculated based on $[Ca^{2+}]_i$ in a compartment. While this model did not include Ca^{2+} buffers, it provides an estimation of the minimum distances and number of channels required to produce KCa1.1 activation. The parameters for Cav2.2 channels were drawn from the studies of references 8, 9, and 11, and Cav3.2 channels from experiments

(data not shown) and reference 10, and KCa1.1 channels from references 6 and 7.

We first compared the activation properties of KCa1.1 by a single Cav3.2 or Cav2.2 channel as a Ca^{2+} source at a fixed distance of 20 nm, which would correspond to direct juxtaposition of a Cav and KCa1.1 channel. Cav3.2 channels have a small single channel conductance (1.7 pS) and exhibit rapid and complete inactivation.^{6,8} At a distance of 20 nm from KCa1.1 in the model, a single Cav3.2 channel only caused a slight increase in the open probability (P_o) of the KCa1.1 channel, reaching just 0.06 of maximal conductance (Fig. 2A, right, dark blue). Cav2.2 channels have a much higher single channel conductance, maximal P_o , and inactivate slowly.^{5,6,10,12} A single Cav2.2 channel at 20 nm distance from a KCa1.1 channel was thus able to increase the KCa1.1 P_o to 0.14, or twice that of a single Cav3.2 channel (Fig. 2A, left).

It has been proposed that multiple Cav channels may complex with KCa1.1 channels, as much as 1 Cav channel per KCa1.1 α -subunit.¹ We also hypothesized that multiple Cav3.2 channels may cooperate to activate KCa1.1 channels.⁴ Indeed, increasing the number of Cav3.2 and Cav2.2 channels in the model (see Methods) resulted in a significant increase in KCa1.1 activation. Thus, a KCa1.1-Cav3.2 complex with 4 Cav3.2 channels at 20 nm distance (KCa1.1-Cav3.2[4; 20 nm]) reached a peak of only 0.49, while a model of 4 Cav2.2 channels complexed

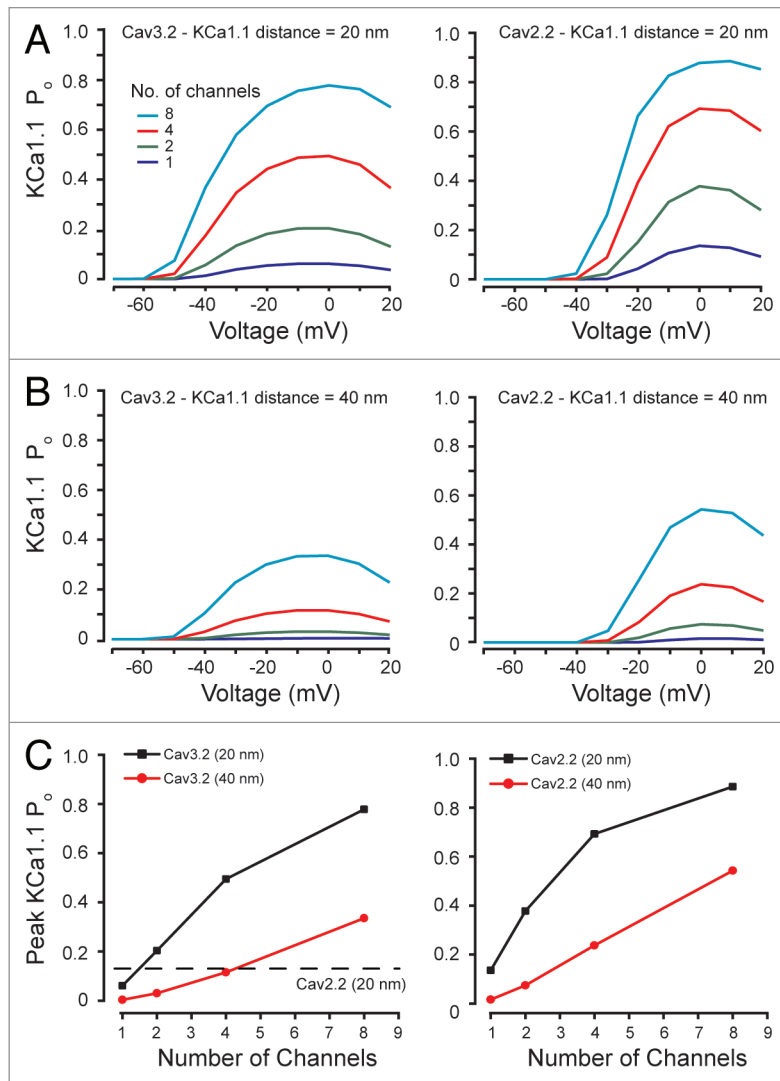


Figure 2. Voltage-dependent properties of KCa1.1-Cav complexes with multiple Cav channels. **(A)** KCa1.1-Cav3.2 and KCa1.1-Cav2.2 complexes exhibit different voltage dependencies. KCa1.1-Cav3.2 complexes (1–8 channels at 20 nm, left) show significant activation in low voltage ranges. KCa1.1-Cav2.2 complexes (1–8 channels at 20 nm, right) only show activation for voltages more positive than -40 mV. KCa1.1-Cav2.2(8; 20 nm) has a greater maximal activation than the KCa1.1-Cav3.2(8; 20 nm) model. **(B)** Increasing the distance between the KCa1.1 and Cav3.2 or Cav2.2 channels to 40 nm significantly decreases the maximal activation of KCa1.1 channels over all voltages. **(C)** Plots of the maximal P_o for Cav3.2 (left) or Cav2.2 (right) channels when different numbers of channels are included in the complex. Dashed line indicates the peak P_o for a single Cav2.2 channel, for reference. KCa1.1-Cav2.2 complexes generate greater KCa1.1 activation when compared with KCa1.1-Cav3.2 complexes with the same number of channels.

with the KCa1.1 channel at 20 nm (KCa1.1-Cav2.2[4; 20 nm]) reached a maximum of 0.69. However, multiple Cav3.2 channels generated significant KCa1.1 activation at voltages as low as -50 mV (Fig. 2A, left). KCa1.1-Cav2.2 complexes, on the other hand, only showed activation for voltages positive to -30 mV (Fig. 2A, right).

Overall, these results show that the higher single channel conductance of a

Cav2.2 channel allows a single channel to be much more effective at activating a nearby KCa1.1 channel than does a Cav3 channel. In fact, multiple Cav3 Ca^{2+} channels are required to provide significant activation of KCa1.1 channels. The voltage-dependence of the Ca^{2+} channel is also reflected in KCa1.1 activation, such that Cav3 channels are capable at activating KCa1.1 channels from lower voltage than Cav2.2 channels.

The distance between the KCa1.1 channel and its Ca^{2+} source is an important factor determining KCa1.1 activation.^{1,5,16-19} Therefore, we tested the effects of increasing the distance between Cav and KCa1.1 channels. At a distance of 40 nm (within a nanodomain), both the KCa1.1-Cav3.2 and KCa1.1-Cav2.2 models showed much weaker activation of KCa1.1 than for a 20 nm separation (Fig. 2B and C). The KCa1.1-Cav3.2(4; 40 nm) complex reached a peak of only 0.12, or 23% of the maximal activation of the KCa1.1-Cav3.2(4; 20 nm) complex (Fig. 2B and C, left). Likewise, the KCa1.1-Cav2.2(4; 40 nm) complex reached a maximum of 0.24 compared with 0.69 at 20 nm separation (Fig. 2B and C, right). Therefore, Ca^{2+} -dependent activation of a KCa1.1-Cav complex depends strongly on interchannel distance and is sensitive to even small differences in separation, with the largest effect on Cav3 as compared with Cav2.2 containing complexes (Fig. 2C).

Cav3.2 and Cav2.2 channels differ significantly in their kinetic properties. Cav3.2 channels show fast activation and a short time constant of inactivation while Cav2.2 channels show inactivation, but to a lesser extent and over a greater timeframe. A series of voltage steps provided to the KCa1.1-Cav3.2(4; 20 nm) model revealed a KCa1.1 channel current that also showed fast activation followed by rapid inactivation within 100 ms. This is important in confirming that the properties of the Cav3 channel were conferred to the KCa1.1 channel (Fig. 3A), as found in MVN neuron and tsA-210 cell recordings.⁴ On the other hand, the KCa1.1-Cav2.2(1; 20 nm) model showed slower inactivation of K^+ current with significant activation still observed after 300 ms (Fig. 3B). As previously reported, no significant activation was detected below -30 mV for the KCa1.1-Cav2.2(1; 20 nm) complex, again confirming direct recordings.¹⁵ Increasing the number of Cav2.2 channels resulted in a slowing of inactivation for the KCa1.1-Cav2.2 complex, which was not seen for an increased number of Cav3.2 channels (Fig. 3C). This is due to the larger conductance of Cav2.2 channels and build-up of $[Ca^{2+}]_i$ with a large number of Cav2.2 channels.

Discussion

The results shown in Rehak et al.⁴ demonstrated a coupling of KCa1.1-Cav3.2 channels in a complex as determined by coimmunoprecipitation of α -subunits, suggesting a nanodomain interaction. This was further supported by a Cav3-dependent activation of KCa1.1 current in the form of a low voltage-activated and fast inactivating KCa1.1 current. The model is also consistent with these results and shows that, when sufficient Ca^{2+} influx is present, the voltage-dependence and kinetics of KCa1.1 channel activation resembles that of an LVA Cav3 Ca^{2+} channel. A similar conferring of voltage-dependence by different HVA Ca^{2+} channels upon KCa1.1 channel activation was previously reported.² Paradoxically, the Cav3 activation of KCa1.1 current could be blocked with as little as 5 mM EGTA, a result usually interpreted as reflecting a microdomain interaction between subunits (reviewed in ref. 5). The modeling results in Rehak et al.⁴ and the current study support experimental results in predicting that multiple Cav3 channels are necessary to cause significant KCa1.1 activation. However, this model simulates an optimal solution where up to 8 Ca^{2+} channels provide Ca^{2+} influx to the intracellular volume immediately surrounding the KCa1.1 channel, which may not be physically feasible (in fact, a 4:1 Cav-KCa1.1 stoichiometry is likely the limit¹). Furthermore, increasing the distance significantly diminished KCa1.1 activation, suggesting that an even greater number of Cav3 channels may be required if the Cav-KCa1.1 distance is increased. Based on the effect of EGTA and the modeling results, we theorize that the Ca^{2+} domains of multiple KCa1.1-Cav3.2 complexes cooperate to provide sufficient increases in $[\text{Ca}^{2+}]_i$ to cause KCa1.1 activation. This cooperation of Ca^{2+} microdomains would be sensitive to slower Ca^{2+} chelators like EGTA, yet still allow for physical association between KCa1.1 and Cav3 channels.

Consistent with published results, models of Cav3 and Cav2.2 channels showed differences in their activation of KCa1.1 channels, reflecting the predicted amount of the Ca^{2+} influx generated by

either channel subtype. The relatively high conductance of the HVA Cav2.2 channel and slow rate of inactivation compared with the low conductance,

fast inactivating Cav3 channel allows Cav2.2 channels to interact with KCa1.1 channels from a farther distance than a Cav3 channel source. In fact, a

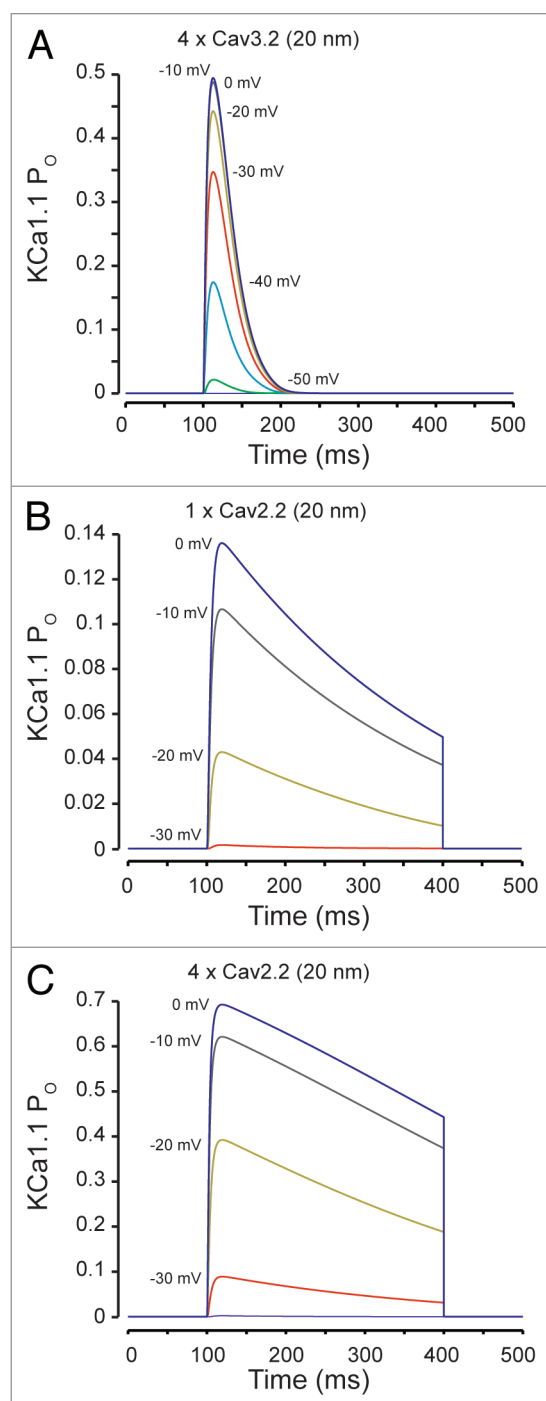


Figure 3. Temporal properties of Cav-KCa1.1 currents. **(A)** A KCa1.1-Cav3.2(4; 20 nm) complex generates a transient current which inactivates within 100 ms. KCa1.1 activation can be observed for voltages over -60 mV. **(B and C)** KCa1.1-Cav2.2 complexes (1 or 4 channels; 20 nm) generate long-lasting KCa1.1 activation with slow inactivation kinetics. When 4 channels are included in the model, the rate of inactivation of KCa1.1 is slowed for depolarized voltages. Significant KCa1.1 activation can only be seen beyond -40 mV, as expected for a K^+ current that follows the voltage-dependence of the HVA Ca^{2+} source.

similar conclusion was drawn for the importance of the conductive properties of a specific Ca^{2+} source capable of activating SK channels when comparing the large conductance NMDA or $\alpha 9/\alpha 10$ nicotinic acetylcholine receptors to that of HVA Ca^{2+} channels.^{1,16-19} In the case of Cav3 Ca^{2+} channels, we interpret this to indicate that the relatively weak and transient T-type Ca^{2+} conductance must increase its effectiveness by creating cooperative microdomains, an association more liable to block by EGTA. The potential for KCa1.1-Cav complexes to cooperate to generate sufficient activation requires further examination and opens the possibility for KCa1.1 regulation by other Ca^{2+} sources which have previously been thought insufficient.

Disclosure of Potential Conflicts of Interest

No potential conflicts of interest were disclosed.

Acknowledgments

This work was supported by operating grants from the Canadian Institutes of Health Research (CIHR) to Turner RW and Zamponi GW. Turner RW and Zamponi GW are Alberta Innovates-Health Solutions (AI-HS) Scientists, Zamponi GW is a Canada Research Chair. Engbers JDT held AI-HS, CIHR, Killam Trust and Dr T Chen Fong studentships. Peer review of this manuscript was handled by Dr Terry Snutch.

References

- Berkefeld H, Fakler B, Schulte U. Ca^{2+} -activated K^{+} channels: from protein complexes to function. *Physiol Rev* 2010; 90:1437-59; PMID:20959620; <http://dx.doi.org/10.1152/physrev.00049.2009>
- Berkefeld H, Fakler B. Repolarizing responses of BKCa-Cav complexes are distinctly shaped by their Cav subunits. *J Neurosci* 2008; 28:8238-45; PMID:18701686; <http://dx.doi.org/10.1523/JNEUROSCI.2274-08.2008>
- Grunnet M, Kaufmann WA. Coassembly of big conductance Ca^{2+} -activated K^{+} channels and L-type voltage-gated Ca^{2+} channels in rat brain. *J Biol Chem* 2004; 279:36445-53; PMID:15210719; <http://dx.doi.org/10.1074/jbc.M402254200>
- Rehak R, Bartoletti TM, Engbers JDT, Berecki G, Turner RW, Zamponi GW. Low voltage activation of KCa1.1 current by Cav3-KCa1.1 complexes. *PLoS One* 2013; 8:e61844; PMID:23626738; <http://dx.doi.org/10.1371/journal.pone.0061844>
- Fakler B, Adelman JP. Control of K(Ca) channels by calcium nano/microdomains. *Neuron* 2008; 59:873-81; PMID:18817728; <http://dx.doi.org/10.1016/j.neuron.2008.09.001>
- van Welie I, du Lac S. Bidirectional control of BK channel open probability by CAMKII and PKC in medial vestibular nucleus neurons. *J Neurophysiol* 2011; 105:1651-9; PMID:21307321; <http://dx.doi.org/10.1152/jn.00058.2011>
- Womack MD, Khodakhah K. Characterization of large conductance Ca^{2+} -activated K^{+} channels in cerebellar Purkinje neurons. *Eur J Neurosci* 2002; 16:1214-22; PMID:12405981; <http://dx.doi.org/10.1046/j.1460-9568.2002.02171.x>
- Jones SW, Marks TN. Calcium currents in bullfrog sympathetic neurons. I. Activation kinetics and pharmacology. *J Gen Physiol* 1989; 94:151-67; PMID:2478659; <http://dx.doi.org/10.1085/jgp.94.1.151>
- Buraci Z, Angheliescu M, Elmslie KS. Slowed N-type calcium channel (CaV2.2) deactivation by the cyclin-dependent kinase inhibitor roscovitine. *Biophys J* 2005; 89:1681-91; PMID:15951378; <http://dx.doi.org/10.1529/biophysj.104.052837>
- Chen CF, Hess P. Mechanism of gating of T-type calcium channels. *J Gen Physiol* 1990; 96:603-30; PMID:2172443; <http://dx.doi.org/10.1085/jgp.96.3.603>
- Lee HK, Elmslie KS. Gating of single N-type calcium channels recorded from bullfrog sympathetic neurons. *J Gen Physiol* 1999; 113:111-24; PMID:9874692; <http://dx.doi.org/10.1085/jgp.113.1.111>
- Weber AM, Wong FK, Tufford AR, Schlichter LC, Matveev V, Stanley EF. N-type Ca^{2+} channels carry the largest current: implications for nanodomains and transmitter release. *Nat Neurosci* 2010; 13:1348-50; PMID:20953196; <http://dx.doi.org/10.1038/nn.2657>
- Koch C, Segev I, eds. *Methods in Neuronal Modeling: From Ions to Networks*. Cambridge: The MIT Press, 1998.
- Prinz AA, Billimoria CP, Marder E. Alternative to hand-tuning conductance-based models: construction and analysis of databases of model neurons. *J Neurophysiol* 2003; 90:3998-4015; PMID:12944532; <http://dx.doi.org/10.1152/jn.00641.2003>
- Berkefeld H, Sailer CA, Bildl W, Rohde V, Thumfart JO, Eble S, Klugbauer N, Reisinger E, Bischofberger J, Oliver D, et al. BKCa-Cav channel complexes mediate rapid and localized Ca^{2+} -activated K^{+} signaling. *Science* 2006; 314:615-20; PMID:17068255; <http://dx.doi.org/10.1126/science.1132915>
- Church PJ, Stanley EF. Single L-type calcium channel conductance with physiological levels of calcium in chick ciliary ganglion neurons. *J Physiol* 1996; 496:59-68; PMID:8910196
- Koh DS, Geiger JR, Jonas P, Sakmann B. Ca^{2+} -permeable AMPA and NMDA receptor channels in basket cells of rat hippocampal dentate gyrus. *J Physiol* 1995; 485:383-402; PMID:7545230
- Plazas PV, De Rosa MJ, Gomez-Casati ME, Verbitsky M, Weisstaub N, Katz E, Bouzat C, Elgoyhen AB. Key roles of hydrophobic rings of TM2 in gating of the $\alpha 9\alpha 10$ nicotinic cholinergic receptor. *Br J Pharmacol* 2005; 145:963-74; PMID:15895110; <http://dx.doi.org/10.1038/sj.bjp.0706224>
- Weisstaub N, Vetter DE, Elgoyhen AB, Katz E. The $\alpha 9\alpha 10$ nicotinic acetylcholine receptor is permeable to and is modulated by divalent cations. *Hear Res* 2002; 167:122-35; PMID:12117536; [http://dx.doi.org/10.1016/S0378-5955\(02\)00380-5](http://dx.doi.org/10.1016/S0378-5955(02)00380-5)